T.R.

BOLU ABANT İZZET BAYSAL UNIVERSITY

INSTITUTE OF GRADUATE STUDIES

Department of Physics

EFFECT OF NOISE ON QUANTUM COHERENCE AND NON-MARKOVIANITY

MASTER OF SCIENCE

NISREEN MOHAMMED MAHDI

ACADEMIC SUPERVISOR

Assist. Prof. Dr. Arzu KURT

BOLU, JANUARY 2023

APPROVAL OF THE THESIS

EFFECT OF NOISE ON QUANTUM COHERENCE AND NON-MARKOVIANITY submitted by **Nisreen MOHAMMED MAHDI** and defended before the Examining Committee Members listed below in partial fulfillment of the requirements for the degree of **MASTER OF SCIENCE in THE DEPARTMENT OF PHYSICS**, Institute of Graduate Studies of Bolu Abant İzzet Baysal University in **09.01.2023** by

Examining Committee Members	**Signature**
Supervisor Assist. Prof. Dr. Arzu KURT Bolu Abant İzzet Baysal University	
Member Prof. Dr. Ferdi ALTINTAŞ Bolu Abant İzzet Baysal University	
Member Assoc. Prof. Dr. Atılgan ALTINKÖK National Defense University	

Prof. Dr. İbrahim KÜRTÜL

Director of Institute of Graduate Studies

ETHICAL DECLARATION

In this thesis dissertation that was properly prepared according to the Thesis Writing Rules of Bolu Abant İzzet Baysal University of the Institute of Graduates Studies, I hereby declare that;

- ▷ All data, information, and documents presented in the thesis were obtained in accordance with the academic and ethical rules,
- ▷ All data, documents, assessments, and results were presented in accordance with the scientific ethical and moral rules,
- ▷ All works that were benefitted in the thesis were appropriately cited,
- ▷ No alteration was made in the data used,
- ▷ Study presented in this thesis is original,

Otherwise, I declare that I accept the loss of all my rights in case any contradiction that may arise against me.

Based on the plagiarism report that was generated on the date of **09/01/2023** by using predetermined filtrations set by Directorate of Institute of Graduate Studies of the Turnitin program, a plagiarism detection software, the similarity index detected was **21%**.

Nisreen MOHAMMED MAHDI

ABSTRACT

EFFECT OF NOISE ON QUANTUM COHERENCE AND NON-MARKOVIANITY

MASTER OF SCIENCE

NISREEN MOHAMMED MAHDI

BOLU ABANT IZZET BAYSAL UNIVERSITY

INSTITUTE OF GRADUATE STUDIES

DEPARTMENT OF PHYSICS

(SUPERVISOR: ASSIST. PROF. DR. ARZU KURT)

BOLU, JANUARY 2023

(ix+40)

In this thesis, we have studied the quantum coherence and non-Markovianity of a two-level system whose energy level is modulated by Gaussian noise, and also its tunneling barrier is fluctuated by a random telegraph noise (RTN). We have investigated the system dynamics by solving the Liouville-von Neumann equation. Using analytical methods, we have obtained the exact solution of the two-level system considered in the thesis for very limited parameter values. We can summarize the important findings of the thesis as follows; (i) for two different initial states, the coherence is found to exhibit damped oscillation behavior, (ii) in the presence of a high Kubo number (K), we discover non-Markovian dynamics, (iii) It is also found that there is no strong relationship between system coherence and non-Markovianity dynamics, with the exception of a region where these two quantities start to change their characters at $K = 1$ for two initial states.

KEYWORDS: Quantum Tunneling, Quantum Coherence, non-Markovianity Measure, Random Telegraph Noise

ÖZET

GÜRÜLTÜNÜN KUANTUM EŞEVRELİLİK VE MARKOVYAN OLMAMA ÜZERİNDEKİ ETKİSİ

FEN BİLİMLERİ

NISREEN MOHAMMED MAHDI

BOLU ABANT İZZET BAYSAL ÜNİVERSİTESİ

LİSANSÜSTÜ EĞİTİM ENSTİTÜSÜ

FİZİK ANABİLİM DALI

(TEZ DANIŞMANI: DR. ÖĞRETİM ÜYESİ ARZU KURT)

BOLU, OCAK - 2023

(ix + 40)

Bu tezde, tünelleme bariyeri bir rastgele telgraf gürültüsü (RTN) ve enerji aralığı ise Gaussian gürültüsü tarafından rahatsız edilen bir kuantum tünelleme sisteminin eşevrelilik ve Markovyan olmama durumunu çalıştık. Sistemin dinamiğini Liouville-von Neumann denklemini çözerek inceledik. Tezde bahsi geçen iki seviyeli sistemin matematiksel çözümü analitik yöntemler kullanılarak çok sınırlı parametre değerleri için elde ettik. Tezin önemli sonuçlarını şu şekilde sıralayabiliriz; (i) iki farklı başlangıç durumları için, eşevrelilik ölçütü $C_{l1}(\rho)$ sönümlü salınım davranışı gösterdiği bulunmuştur, (ii) Markovyan olmayan dinamikler Kubo K sayısının yüksek olduğu durumda gözlemlenmiştir, (iii) sistemin eşevreliliği ile Markovyan olmayan dinamikler arasında, bu iki niceliğin her iki başlangıç durumları için davranışlarını değiştirme eğiliminde olduğu $K = 1$ bölgesi dışında, güçlü bir ilişki olmadığı da bulunmuştur.

ANAHTAR KELİMELER: Kuantum Tünellemesi, Kuantum Eşevrelilik, Markovyan Olmayan Ölçüt, Rastgele Telgraf Gürültüsü

TABLE OF CONTENTS

LIST OF FIGURES

ACKNOWLEDGEMENTS

Thank you, Lord, for giving me the strength, patience, and determination to complete my thesis and achieve my dream. I express my deepest gratitude to my supervisor Dr. Arzu Kurt, and co-supervisor Dr. Ferdi Altintas; for their guidance, advice, criticism, encouragement, and insights throughout the research.

I dedicate my achievement and thesis to those who worked hard for me and stood by me, to my beloved mother, beloved father, dear sisters, and great-grandfather. I dedicate it to my friends. You were my best supporter. Your presence is essential in all my successes. I also dedicate it to my friend Ahmed Saeed and Omar Al-Ani. With you, my friends, I completed my thesis. Finally, thanks to myself, who got sick and tired and broke down, I didn't give up. Thank you, Nisreen.

I also acknowledge my recently submitted manuscript entitled "Nisreen Mohammed Mahdi, Arzu Kurt, and Ferdi Altintas, Quantum Coherence and non-Markovianity in a Noisy Quan- tum Tunneling Problem. arXiv:2208.07947 (2022)", which is a part of this thesis and presented in the result and discussion section (4).

LIST OF ABBREVIATIONS AND SYMBOLS

TLS : Two Level System

RTN : Random Telegraph Noise

$\boldsymbol{\Delta}$: Tunneling Matrix Element

$\boldsymbol{\Omega}$: Noise Amplitude

ϵ : Level Energy Difference

H : Hamiltonian

$\hbar$: Planck's constant

$\sigma_{\mathbf{x,y,z}}$: Pauli Matrix

$\mathcal{I}$: Identity Operator

η : White Noise Intensity

ν : Noise Frequency

$\mathbf{C_{l_1}}$: l_1-norm of Coherence

$\mathbf{C_{rel.net}}$: Relative Entropy

$S(\rho)$: Liouville-von Neumann Entropy

$\mathcal{N}$: Measure of Non-Markovianity

ξ : Gaussian Noise

U : Unitary Evolution Operator

K : Kubo Number

ρ : Density Matrix Operator

κ : System-Environment Interaction Strength

INTRODUCTION

Understanding and controlling the two-level system–the simplest quantum system–plays a critical role in advancing quantum technologies [1]. Quantum tunneling has essential applications, for example, in nanotechnology, tunnel diodes, quantum computing, and scanning electron microscopy [2, 3, 4]. The tunneling effect may also restrict some nanotechnology devices' minimum size and functioning [2, 3, 4].

The two-level system gives the simplest description of quantum tunneling [5, 6]. Whereby only the lowest two energy levels are well localized. The two-level approximation makes sense when the energies of the two localized levels are much smaller than the higher energy levels and the height of the barrier. When the system is isolated, only two parameters are sufficient to describe the quantum tunneling problem. The first one is the tunneling matrix element Δ which couples the two effective energy levels and gives information about the barrier height. The other is the bias parameter ϵ, which offers the energy difference between the two lowest energy levels. The bias parameter also corresponds to the measure of the asymmetry of the system. On the other hand, quantum systems are unavoidably exposed to environmental noise or external perturbations, which leads to dissipation and decoherence [5, 6, 7]. Here, we model the open system leading to a stochastic energy bias $\epsilon(t)$ and the barrier to random fluctuations, $\Delta(t)$ [5].The tunneling problem with time-dependent bias and barriers has been focused on in a number of studies [8, 9, 10, 11, 12, 13, 14, 15, 16]. The studies [9, 10] have exposed the tunneling system to external fields, for example, to a strong laser field, which results in the time dependence of the bias, $\epsilon(t)$. On the other hand, the studies [8, 11, 12, 13, 14, 15, 16] have also considered the barrier parameter $\Delta(t)$ to be time-dependent by either driving the barrier with periodic signals or exposing it to a stochastic perturbation. The tunneling problem with time-modulated parameters has been known to occur in several physical situations, for example, long-range electron transfer reactions [17, 18], some problems in semiconductor physics [19], polarization of a multilayer structure [20, 21] and the scattering problem [22, 23].

In the present study, we focus on the same problem of quantum tunneling in the presence of a stochastic bias and a fluctuating barrier under the two-level approximation. We consider here that the fluctuations in the barrier are induced by dichotomous noise, while coupling to a high-temperature reservoir causes the dissipation of the bias. The correlation time of barrier fluctuations has been studied in relation to tunneling dynamics between two localized energy levels [5]. Resonant damping of tunneling has been observed due to noise in the system. On the other hand, our main interest is to analyze the dependence of quantum coherence dynamics on the correlation time of the barrier fluctuations and elucidate its non-Markovian character.

Quantum coherence is one of the unique features of quantum mechanics, indicating the capability of a state to exhibit quantum interference effects. Other quantum properties such as quantum entanglement, non-locality, discord, and steering are essentially quantum mechanical properties. Quantum coherence plays an instrumental role in the protocols of quantum information and computation [24], and also in the emergent areas, such as quantum thermodynamics [25], biology [26], and metrology [27]. Only very recently, a rigorous theory for measuring quantum coherence has been proposed to use coherence as a physical resource [28, 30]. After development, its intimate connection to entanglement and quantum correlations has been given in [31, 32, 33, 34, 35]. Besides, properties such as freezing and distillation of coherence have been investigated in Refs. [30, 36, 37, 38]. The non-Markovian effect, on the other hand, is a quantum mechanical effect that reflects the environment back onto quantum systems. Exploring non-Markovian features can be helpful in the fabrication of nano-scale machines [39, 40, 41, 42, 43, 44]. In the context of quantum thermodynamics, non-Markovianity is used as an extra fuel to supply a quantum thermal machine [43, 44]. Along similar lines, a measure for the degree of non-Markovianity, which accounts for non-zero values for information flow back to the system, has been given very recently [45, 46]. Using the aforementioned quantifiers, we analyze the quantum coherence dynamics in terms of the barrier parameters and show the non-Markovian character of the barrier fluctuations. We show here that both measures display special structures at specific system parameters. Since we consider the tunneling problem with well-defined discrete energy levels, it is reasonable to discuss quantum coherence between localized energy states and their suppression due to noise in the barrier and bias.

The outline of the thesis is organized in the following way. We introduce the mathematical tools for the noisy two-level system in chapter 2 that includes the noise properties we use in the thesis and also presents the quantum measures. In chapter 3 we present the set of solutions of the averaging over Gaussian noise as well as the RTN signal of the models. The main results of the thesis are discussed accordingly to the models in chapter 4 and finally, we conclude with a summary of the main results in chapter 5.

MATHEMATICAL TOOLS FOR NOISY TWO-LEVEL SYSTEMS

In this chapter, we present how the dynamics of the two-level system evolve in time in the absence of external noise by associating with the population difference and quantum coherence quantities. We then introduce the characterization of the noises used in the thesis and the definition of quantum measures at the end.

2.1 Two-Level System

We consider a two-level system which is described by the following Hamiltonian:

$$H = \frac{\hbar\,\epsilon}{2}\sigma_z, \tag{2.1}$$

where σ_z is the Pauli matrix and $\hbar\epsilon$ is the energy difference between two levels.

The dynamics of the system describe the Hamiltonian in the equation (2.1) is governed by the Liouville-von Neumann equation:

$$\frac{d\,\rho}{dt} = -\frac{i}{\hbar}\left[H, \rho\right], \tag{2.2}$$

where $[A, B] = A \cdot B - B \cdot A$ is the commutator of operators A and B. We will find the commutator of the Hamiltonian and the density operator and use it in the Liouville-von Neumann equation (2.2):

$$\begin{aligned} \frac{d\rho}{dt} &= -\frac{i}{\hbar}\left[\begin{pmatrix} \hbar\,\epsilon/2 & 0 \\ 0 & -\hbar\,\epsilon/2 \end{pmatrix}, \begin{pmatrix} \rho_{11} & \rho_{12} \\ \rho_{21} & \rho_{22} \end{pmatrix}\right] \\ &= \begin{pmatrix} 0 & -i\,\epsilon\rho_{12} \\ i\,\epsilon\rho_{21} & 0 \end{pmatrix}. \end{aligned} \tag{2.3}$$

One can see from equation (2.3) that the diagonal elements of the density matrix are constant, while the off-diagonal elements, called coherence, change at a rate proportional to the transition energy ϵ of the system. The components of the Bloch vector of the system are defined from the density matrix– $\rho = \left(I + \sum_i P_i \sigma_i\right)/2$– where σ_i are the Pauli matrices, $i = x, y, z$, I is the identity operator, and P_i are the components of the Bloch vector. This means that the population difference is $P_z = \langle\sigma_z\rangle = \rho_{11} - \rho_{22}$ and the real and complex components of the coherence term are $P_x = \langle\sigma_x\rangle = (\rho_{12} + \rho_{21})/2$ and $P_y = \langle\sigma_y\rangle = i(\rho_{12} - \rho_{21})/2$, respectively. Based on equation (2.3) in the form of the Bloch vector equation, one can obtain the set of first-order coupled differential equations:

$$\begin{aligned}
\dot{P}_z(t) &= 0 \\
\dot{P}_x(t) &= -\epsilon\, P_y(t) \\
\dot{P}_y(t) &= \epsilon\, P_x(t),
\end{aligned} \tag{2.4}$$

where $\dot{\mathcal{O}}$ indicates the first order derivation of $\mathcal{O}$ in terms of time. It is obvious that the population difference is constant in time, while the coherence terms $P_x(t)$ and $P_y(t)$ depend on each other, which means that they oscillate with the frequency ϵ if there is any initial coherence in the system.

We now generalize the model by adding a tunneling term Δ which would allow one to couple the two states of the system and its Hamiltonian is given by:

$$H = \frac{\hbar\,\epsilon}{2}\sigma_z + \frac{\hbar\,\Delta}{2}\sigma_x, \tag{2.5}$$

where ϵ is the energy difference between two levels, while Δ is the tunneling matrix element of the system. It is straightforward to obtain the solution by using the Liouville-von Neumann equation in equation (2.2):

$$\begin{aligned} \frac{d\rho}{dt} &= -\frac{i}{\hbar}\left[\begin{pmatrix} \hbar\,\epsilon/2 & \hbar\,\Delta/2 \\ \hbar\,\Delta/2 & -\hbar\,\epsilon/2 \end{pmatrix}, \begin{pmatrix} \rho_{11} & \rho_{12} \\ \rho_{21} & \rho_{22} \end{pmatrix}\right] \\ &= \begin{pmatrix} i\,\Delta(\rho_{21}-\rho_{12})/2 & -i\,\epsilon\,\rho_{12}+i\,\Delta(\rho_{11}-\rho_{22})/2 \\ i\,\epsilon\,\rho_{21}-i\,\Delta(\rho_{11}-\rho_{22})/2 & -i\,\Delta(\rho_{12}-\rho_{21})/2 \end{pmatrix} \end{aligned} \tag{2.6}$$

Based on the equation (2.6), one can obtain the set of equation family:

$$\begin{aligned} \dot{P}_z(t) &= \Delta\,P_y(t), \\ \dot{P}_x(t) &= -\epsilon\,P_y(t), \\ \dot{P}_y(t) &= \epsilon\,P_x(t) - \Delta\,P_z(t). \end{aligned} \tag{2.7}$$

As can be seen from the set of equation (2.6), population difference and coherence along x-direction depends on coherence along-y direction with the rate of Δ and ϵ, respectively. However, coherence along-y direction changes with $P_x(t)$ and $P_z(t)$.

2.2 Noise

In this section, we introduce the noises affecting TLS dynamics as well as their correlation functions. We first start with the Gaussian noise–a random signal–whose probability density function obeys the Gaussian distribution. In the thesis, however, we use a special case of Gaussian noise –Gaussian white noise with zero means–in which its amplitude values at any two points in time are uniformly distributed and statistically independent i.e., it has uncorrelated characteristics. We display an example of a Gaussian white noise signal with zero mean-$\mu = 0$-and standard deviation (σ) is equal to 4–$\sigma = 4$–in figure (2.1-a) and its probability density function figure (2.1-b). The yellow histogram depicts the empirical probability density for a sample size of 1000, while the blue line shows the theoretical correspondence. White noise is named after white light, which has a flat power spectrum, which refers to the Fourier transform of the auto-correlation function of the noise, at all frequencies. So, the noise we plot in the figure (2.1-a) whose the auto-correlation function is the delta-correlated function as can be seen from figure (2.2-a). The power spectrum of a signal is how much strength of the signal is at the given frequency. Its spectrum of Gaussian white noise–$S(\omega)$–is plotted in figure (2.2-b). It is found that as expected $S(\omega)$ is constant at all ω's.

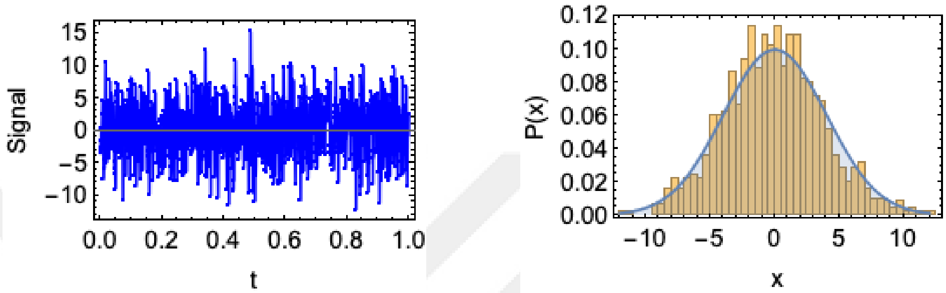

(a) (b)

Figure 2.1: Gaussian white noise signal with zero mean-$\mu = 0$-and standard deviation–$\sigma = 4$–(a) and its probability density function $P(x)$ (b)

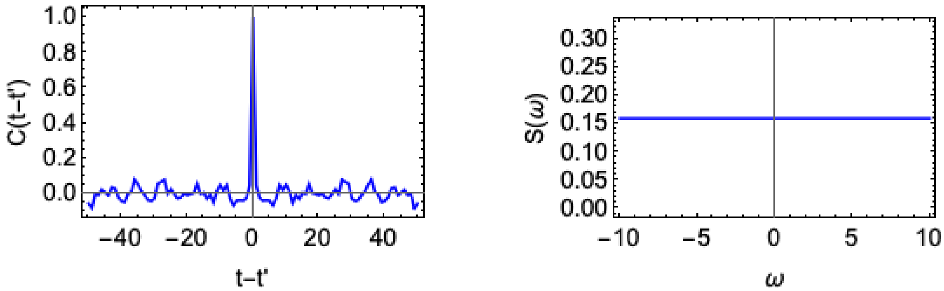

(a) (b)

Figure 2.2: Correlation function $C(t-t')$ of Gaussian white noise as function of time difference $t-t'$ (a) and its power spectrum $S(\omega)$ (b).

Another noise used in the thesis is random telegraph noise, which is considered a non-equilibrium one. In contrast to equilibrium noise, a harmonic thermal bath (Gaussian noise) has been used to describe more natural environments in many studies and in different aspects. For instance, RTN-like disturbances in photosynthetic complexes, such as side-chain rotation and the conformational motion of the protein scaffold [69] for the different protein motions, Ref. [72] for the noisy character of those motions and Ref. [73] for the possibility of modeling those noises as RTN.

Such noise is a dichotomic process that flips between two possible values $+1$ and -1 with a frequency ν and is characterized by the following fundamental properties: zero mean–$\langle \eta(t) \rangle = 0$–and the exponential auto-correlation function–$C(t-t') = \langle \eta(t)\eta(t') \rangle = e^{-2\nu|t-t'|}$–where the inverse of ν relates to the correlation time of the noise. Figure (2.3-a) displays an RTN signal with the switching frequency $\nu = 1$ in the time $t \in [0, 10]$ and the auto-correlation function of such a noise as expected shows the exponential function in the absolute time difference $|t - t'|$ as can be seen from the figure (2.3-b).

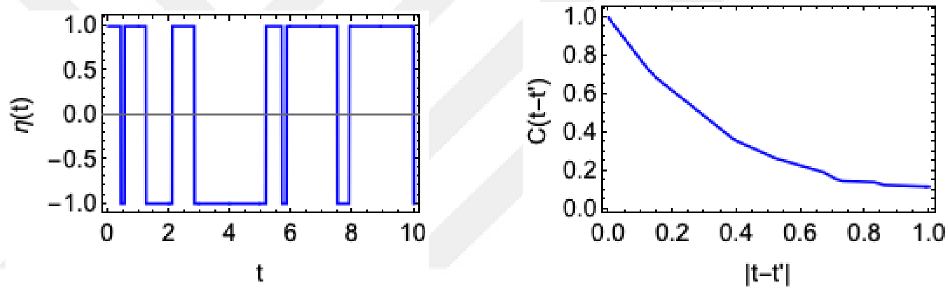

(a) (b)

Figure 2.3: Random telegraph noise with the flipping frequency $\nu = 1$ in the time interval $t \in [0, 10]$ (a) and its auto-correlation function $C(t - t')$.

2.3 Quantum Measures

2.3.1 Measure of Quantum Coherence and Quantum Relative Entropy

A complete theory for the quantification of quantum coherence has been given very recently based on the conditions in analogy to the entanglement theory [28, 29, 30]. The fundamental goal of such an endeavor is to leverage quantum coherence as a beneficial resource in quantum information and computing protocols. The distance between two quantum states, ρ and σ is quantified using a valid metric, $\Delta(\rho||\sigma)$. It is possible to write it as [28]:

$$C_{\Delta}(\rho) = \min_{\sigma \in I} \Delta(\rho||\sigma). \tag{2.8}$$

Here $\sigma = \sum_{i=1}^{d} \sigma_{ii}|i\rangle\langle i|$ is the density operator in the space I representing the incoherent quantum states defined in terms of a particular fixed basis $|i\rangle$–in our case, the eigenstates of σ_z are chosen as the fixed basis. For a given metric $\Delta(\rho||\sigma)$, $C_{\Delta}(\rho)$ determines the minimal distance between the coherent state ρ and the set of all incoherent quantum states defined in the subspace I. Refs. [28, 29, 30] set the necessary conditions to qualify $C_{\Delta}(\rho)$ as a coherence monotone. It has been demonstrated that not all metrics become a proper coherence measure [28, 29, 30, 64, 65]. On the other hand, l_1-matrix norm $\Delta_{l1}(\rho||\sigma) = ||\rho - \sigma||_{l_1} = \Sigma_{ij}|\rho_{ij} - \sigma_{ij}|$ and the relative entropy $\Delta_{rel.ent}(\rho||\sigma) = \mathrm{Tr}(\rho \log_2 \rho - \rho \log_2 \sigma)$ have been shown to satisfy all the requirements for qualifying $C_{\Delta}(\rho)$ as a coherence measure. Furthermore, the minimum in equation (2.8) for both metrics can be obtained for the diagonal density operator $\sigma \equiv \rho_{diag} = \sum_i \rho_{ii}|i\rangle\langle i|$, where $\rho_{ii} = \langle i|\rho|i\rangle$. Therefore, the quantifiers which are called the l_1-norm of coherence–$C_{l_1}(\rho)$– and the relative entropy of coherence–$C_{rel.ent}(\rho)$– have the explicit forms [28]:

$$\begin{aligned} C_{l_1}(\rho) &= \sum_{i \neq j} |\rho_{ij}|, & (2.9) \\ C_{rel.ent}(\rho) &= S(\rho_{diag}) - S(\rho), & (2.10) \end{aligned}$$

where $S(\rho) = -\mathrm{Tr}(\rho \log_2 \rho)$ is the Liouville-von Neumann entropy. It is worth noting that in our calculations we have observed that $C_{l_1}(\rho)$ and $C_{rel.ent.}(\rho)$ give qualitatively the same predictions. Therefore, we will restrict our attention to only $C_{l_1}(\rho)$. Furthermore, the l_1 norm of coherence serves as a very intuitive quantification of coherence, since it is directly connected to the off-diagonal elements of ρ in a fixed basis $|i\rangle$. Recently, some established coherence monotones based on different metrics, such as the (modified) trace norm and fidelity, have been found to be increasing functions of $C_{l_1}(\rho)$ [65, 66, 67]. Non-zero $C_{l_1}(\rho)$ is an indication of quantum interference phenomena between two localized potential wells which are represented by the eigenstates of σ_z. The role of the barrier and its fluctuations in this phenomenon will be investigated for two initial states; one of them is the incoherent state $\rho_1(0) = |1\rangle\langle 1|$ where the particle is localized in one of the wells and the other is the maximal coherent one $\rho_2(0) = |\psi(0)\rangle\langle\psi(0)|$ where $|\psi(0)\rangle = (|1\rangle + i\,|0\rangle)\,/\sqrt{2}$.

2.3.2 Non-Markovianity Measure

The quantification of the degree of non-Markovianity is also based on a metric that requires contraction under all completely positive trace-preserving maps. The trace distance might serve this purpose, which is given as [24]:

$$\Delta_{tr}(\rho_1||\rho_2) = \frac{1}{2}\mathrm{Tr}\,|\rho_1 - \rho_2|\,, \tag{2.11}$$

where $|A| = \sqrt{A^\dagger\,A}$. Based on the trace distance, the measure of non-Markovianity is defined as [45, 46]:

$$\mathcal{N} = \max_{\rho_1,\rho_2} \int_{\sigma>0} \sigma(t)\,dt, \tag{2.12}$$

where $\sigma(t) = \frac{d}{dt}\Delta_{tr}(\rho_1||\rho_2)$. Such quantification is based on the distinguishability of quantum states. Markovian dynamics can always be represented by a dynamical semigroup which is completely positive and trace-preserving. Under Markovian dynamics, the trace distance always contracts, demonstrating the reduction of distinguishability between two arbitrary quantum states. The flow of information is then considered outside the system of interest. The rate of change of $\sigma(t)$ is negative, with the result that $\mathcal{N}$ in equation (2.12) is zero. On the other hand, non-Markovian dynamics can not be described by any completely positive and trace-preserving map. In a map of this kind, the distinguishability of two arbitrary states may increase for some time interval, indicating the flow of information back to the system. In this time domain,

$\sigma(t) > 0$. Please note that the non-Markovianity measure in equation (2.12) accounts for the whole regions where $\sigma(t) > 0$. Therefore, if $\mathcal{N} > 0$, then the dynamics is always non-Markovian. In general, a numerical discretization method is employed over the overall pair of initial states to determine non-Markovianity. Instead, in our calculations, choosing the orthogonal pair $\rho_1(0)$ and $\rho_3(0) = |0\rangle\langle 0|$ would be sufficient to show the non-Markovian character that arises in our framework [45, 46].

AVERAGING OVER NOISE OF DRIVEN TWO-LEVEL SYSTEM

We here report the results of the averaged time evolution equation of a driven two-level system carried out over the Gaussian noise and RTN signal by using the Liouville-von Neumann equation. For the model modulated by Gaussian noise, we take the partial trace over the noise of the von-Neumann equation, while we use the Bourret-Frisch [63] and Loginov-Shapiro theorem [62] to allow us to obtain a factorization for the correlation function of the dichotomous process and to take the average of the time evolution operator of the random telegraph noise, respectively.

3.1 Driven Two-Level System: Gaussian Noise

We consider a system whose energy levels are modulated by time-dependent Gaussian noise $\xi(t)$ and the system Hamiltonian contains constant and time-dependent terms:

$$\begin{aligned} H &= H_0 + H_I(t) \\ &= \frac{\hbar\epsilon}{2}\sigma_z + \frac{\hbar\xi(t)}{2}\sigma_z, \end{aligned} \tag{3.1}$$

where $H_0 = \frac{\hbar}{2}\epsilon\sigma_z$ is the bare system Hamiltonian and $H_I(t) = \frac{\hbar}{2}\xi(t)\sigma_z$ indicates time-dependent Hamiltonian of the two-level system. Here $\xi(t)$ is the Gaussian white noise process and which can be characterized by zero averaging $\langle\epsilon(t)\rangle = 0$ and delta-auto correlation function $\langle\xi(t)\xi(t^{'})\rangle = 4\kappa\delta(t-t^{'})$ in which κ is the indication of the interaction of the system to the environment. Since the Hamiltonian in equation (3.1) consists of a stochastic fluctuation term, we transform H into the interaction picture so that one can isolate the effect of the Gaussian noise $\xi(t)$ term. In the interaction picture, system quantities can be given as:

$$H_I(t) = U^\dagger(t) H(t)\, U(t), \tag{3.2}$$

$$\rho_I(t) = U^\dagger(t)\, \rho(t)\, U(t), \tag{3.3}$$

where $U(t) = \mathcal{T} e^{-\frac{i}{\hbar}\int_0^t d\tau\, H_0(\tau)}$ is the unitary transformation operator with the time ordering term $\mathcal{T}$. The dynamics of the density matrix $\rho_I(t)$ in the interaction picture is governed by

$$\frac{d}{dt}\rho_I(t) = -\frac{i}{\hbar}\left[H_I(t), \rho_I(t)\right]. \tag{3.4}$$

In order to solve such a system one can take a formal integral an both sides of equation (3.4)

$$\int_0^t d\,\rho_I(t) = -\frac{i}{\hbar}\int_0^t dt_1 \left[H_I(t_1), \rho_I(t_1)\right], \tag{3.5}$$

After taking the integral, the solution of $\rho_I(t)$ is easily found as follows:

$$\rho_I(t) = \rho_I(0) - \frac{i}{\hbar}\int_0^t dt_1 \left[H_I(t_1), \rho_I(t_1)\right]. \tag{3.6}$$

Plugging equation (3.6) into equation (3.4) one can read:

$$\frac{d\,\rho_I(t)}{dt} = -\frac{i}{\hbar}[H_I(t), \rho(0)] - \frac{1}{\hbar^2}\int_0^t dt_1 [H_I(t), [H_I(t_1), \rho_I(t_1)]], \tag{3.7}$$

where since $H_I(t) = \hbar\xi(t)\sigma_z/2$ includes Gaussian noise term, one should take an average over the noise. It is given by

$$\langle\frac{d\,\rho_I(t)}{dt}\rangle = -\frac{i}{\hbar}\langle[H_I(t), \rho_I(0)]\rangle - \frac{1}{\hbar^2}\langle\int_0^t dt_1 [H_I(t), [H_I(t_1), \rho_I(t_1)]]\rangle. \tag{3.8}$$

Here $\langle\dots\rangle$ represents the averaging over the noise realization. We will present and compute each term in equation (3.8) below. One can easily show that the average of the unitary term over the degree of freedom of environment is zero–see the first term of equation (3.8)–, which is given by

$$
\begin{aligned}
-\frac{i}{\hbar}\langle[H_I(t),\rho_I(0)]\rangle &= -\frac{i}{\hbar}\langle[\frac{\hbar}{2}\xi(t)\sigma_z\rho_I(t)-\rho_I(t)\frac{\hbar}{2}\xi(t)\sigma_z]\rangle \\
&= -\frac{i}{2}\sigma_z\rho_I(t)\langle\xi(t)\rangle+\frac{i}{2}\rho_I(t)\sigma_z\langle\xi(t)\rangle \\
&= 0
\end{aligned} \tag{3.9}
$$

It is obvious to show that equation (3.9) is zero because of zero averaging Gaussian noise i.e.,$\langle\xi(t)\rangle = 0$. Here if one can consider the time-convolution-less (non-local) master equation for the simplicity [57], which means $\rho_I(t_1) \rightarrow \rho_I(t)$, then the second term of equation (3.8) can be averaged as follows:

$$
\begin{aligned}
-\frac{1}{\hbar^2}\langle\int_0^t dt_1[H_I(t),[H_I(t_1),\rho_I(t_1)]]\rangle &= -\frac{1}{\hbar^2}\langle\int_0^t dt_1[H_I(t),[H_I(t_1),\rho_I(t)]]\rangle \\
&= -\frac{1}{\hbar^2}\int_0^t dt_1\langle H_I(t)H_I(t_1)\rho_I(t)\rangle \\
&\quad +\frac{1}{\hbar^2}\int_0^t dt_1\langle H_I(t)\rho_I(t)H_I(t_1)\rangle \\
&\quad +\frac{1}{\hbar^2}\int_0^t dt_1\langle H_I(t_1)\rho_I(t)H_I(t)\rangle \\
&\quad -\frac{1}{\hbar^2}\int_0^t dt_1\langle\rho_I(t)H_I(t_1)H_I(t)]\rangle
\end{aligned} \tag{3.10}
$$

It is important to note that the above equation (3.10) has four terms that we carry out separately and then substitute the Hamiltonian value into the interaction picture in each part in the following way:

$$
\begin{aligned}
-\frac{1}{\hbar^2}\int_0^t dt_1\langle H_I(t)H_I(t_1)\rho_I(t)\rangle &= -\frac{1}{\hbar^2}\int_0^t dt_1\langle\, U^\dagger(t)\frac{\hbar}{2}\xi(t)\sigma_z\, U(t)\, U^\dagger(t_1)\frac{\hbar}{2}\xi(t_1)\sigma_z\, U(t_1)\rho_I(t)\rangle \\
&= -\frac{1}{4}\int_0^t dt_1\, U^\dagger(t)\sigma_z\, U(t)\, U^\dagger(t_1)\,\sigma_z\, U(t_1)\rho_I(t)\,\underbrace{\langle\xi(t)\xi(t_1)\rangle}_{\downarrow} \\
&= -\frac{1}{4}\int_0^t dt_1\, U^\dagger(t)\sigma_z\, U(t)\, U^\dagger(t_1)\,\sigma_z\, U(t_1)\rho_I(t)\,\overbrace{4\,\kappa\,\delta(t-t_1)} \\
&= -\kappa\; \underbrace{U^\dagger(t)\;\overbrace{\sigma_z\;\underbrace{U(t)\,U^\dagger(t)}_{\mathcal{I}}\;\sigma_z}^{1}\;U(t)}_{\mathcal{I}}\,\rho_I(t) \\
&= -\kappa\,\rho_I(t) \qquad (3.11) \\
\frac{1}{\hbar^2}\int_0^t dt_1\langle H_I(t)\rho(t)H_I(t_1)\rangle &= \frac{1}{\hbar^2}\int_0^t dt_1\langle\, U^\dagger(t)\frac{\hbar}{2}\xi(t)\sigma_z\, U(t)\,\rho_I(t)\, U^\dagger(t_1)\,\frac{\hbar}{2}\xi(t_1)\,\sigma_z\, U(t_1)\rangle \\
&= \frac{1}{4}\int_0^t dt_1\, U^\dagger(t)\sigma_z\, U(t)\,\rho_I(t)\, U^\dagger(t_1)\,\sigma_z\, U(t_1)\langle\xi(t)\,\xi(t_1)\rangle \\
&= \frac{1}{4}\int_0^t dt_1\, U^\dagger(t)\sigma_z\, U(t)\,\rho_I(t)\, U^\dagger(t_1)\,\sigma_z\, U(t_1)\,4\kappa\,\delta(t-t_1) \\
&= \kappa\, U^\dagger(t)\sigma_z\, U(t)\,\rho_I(t)\, U^\dagger(t)\,\sigma_z\, U(t) \qquad (3.12) \\
\frac{1}{\hbar^2}\int_0^t dt_1\langle H_I(t_1)\,\rho(t)\,H_I(t)\rangle &= \frac{1}{\hbar^2}\int_0^t dt_1\langle U^\dagger(t_1)\frac{\hbar}{2}\xi(t_1)\sigma_z\, U(t_1)\,\rho_I(t)\, U^\dagger(t)\,\frac{\hbar}{2}\xi(t)\,\sigma_z\, U(t)\rangle \\
&= \frac{1}{4}\int_0^t dt_1 U^\dagger(t_1)\sigma_z\, U(t_1)\,\rho_I(t)\, U^\dagger(t)\,\sigma_z\, U(t)\langle\xi(t_1)\,\xi(t)\rangle \\
&= \frac{1}{4}\int_0^t dt_1 U^\dagger(t_1)\sigma_z\, U(t_1)\,\rho_I(t)\, U^\dagger(t)\,\sigma_z\, U(t)\,4\kappa\,\delta(t-t_1) \\
&= \kappa\, U^\dagger(t)\sigma_z\, U(t)\,\rho_I(t)\, U^\dagger(t)\,\sigma_z\, U(t) \qquad (3.13) \\
-\frac{1}{\hbar^2}\int_0^t dt_1\langle\rho_I(t)H_I(t_1)H_I(t)]\rangle &= -\frac{1}{\hbar^2}\int_0^t dt_1\langle\rho_I(t)\, U^\dagger(t_1)\frac{\hbar}{2}\xi(t_1)\sigma_z\, U(t_1)\, U^\dagger(t)\,\frac{\hbar}{2}\xi(t)\,\sigma_z\, U(t)\rangle \\
&= -\frac{1}{4}\int_0^t dt_1\rho_I(t)\, U^\dagger(t_1)\sigma_z\, U(t_1)\, U^\dagger(t)\,\sigma_z\, U(t)\langle\xi(t_1)\xi(t)\rangle \\
&= -\kappa\,\rho_I(t) \qquad (3.14)
\end{aligned}
$$

The obtained results from equations (3.11)-(3.14) and equation (3.8) allow us to obtain the master equation equation (3.10) in the interaction picture as follows:

$$
\begin{aligned}
\langle \frac{d\,\rho_I(t)}{dt} \rangle &= -2\kappa\,\rho_I(t) + 2\kappa\,U^\dagger(t)\sigma_z\,U(t)\,\rho_I(t)\,U^\dagger(t)\sigma_z\,U(t) \\
&= 2\kappa\,U^\dagger(t)(\sigma_z\rho(t)\sigma_z - \rho(t))U(t). \qquad (3.15)
\end{aligned}
$$

Since the master equation in equation (3.15) is in the interaction picture, we need to transfer it to its original frame–Shrödinger picture–by utilizing the relation $\rho_I(t) = U^\dagger(t)\,\rho(t)\,U(t)$ in equation (3.3) and taking the derivative of $\rho_I(t)$ in terms of t i.e.,

$$
\frac{d}{dt}\rho_I(t) = \frac{dU^\dagger(t)}{dt}\rho(t)U(t) + U^\dagger(t)\frac{d\rho(t)}{dt}U(t) + U^\dagger\rho(t)\frac{dU(t)}{dt}, \quad (3.16)
$$

where the derivative of $U^\dagger(t)$ and $U(t)$ in terms of t can be computed readily based on the definition of the unitary operator:

$$
\begin{aligned}
U(t) &= \mathcal{T}e^{-\frac{i}{\hbar}\int_0^t d\tau\,H(\tau)} \rightarrow \quad \frac{dU(t)}{dt} = -\frac{i}{\hbar}H(t)U(t), \qquad (3.17) \\
U^\dagger(t) &= \mathcal{T}e^{\frac{i}{\hbar}\int_0^t d\tau\,H(\tau)} \rightarrow \quad \frac{dU^\dagger(t)}{dt} = \frac{i}{\hbar}H(t)U(t). \qquad (3.18)
\end{aligned}
$$

Plugging equation (3.17)-(3.18) into equation (3.16) gives:

$$
\begin{aligned}
\frac{d\rho_I(t)}{dt} &= \frac{i}{\hbar}U^\dagger(t)H_0(t)\rho(t)U(t) - \frac{i}{\hbar}U^\dagger(t)\rho(t)H_0(t)U(t) \\
&+ U^\dagger(t)\frac{d\rho(t)}{dt}U(t) \\
&= \frac{i}{\hbar}U^\dagger(t)[H_0(t),\rho(t)]U(t) + U^\dagger\frac{d\rho(t)}{dt}U(t). \qquad (3.19)
\end{aligned}
$$

We now equalize equation (3.15) with equation (3.19) and use equation (3.3), one can obtain as follows:

$$
\begin{aligned}
\frac{i}{\hbar}U^\dagger(t)[H_0(t),\rho(t)]U(t) + U^\dagger\frac{d\rho(t)}{dt}U(t) &= 2\kappa\,U^\dagger(t)(\sigma_z\rho(t)\sigma_z - \rho(t))U(t) \\
\frac{i}{\hbar}\cancel{U^\dagger(t)}[H_0(t),\rho(t)]\cancel{U(t)} + \cancel{U^\dagger(t)}\frac{d\rho(t)}{dt}\cancel{U(t)} &= 2\kappa\,\cancel{U^\dagger(t)}(\sigma_z\rho(t)\sigma_z - \rho(t))\cancel{U(t)}
\end{aligned}
$$

After deleting $U^\dagger(t)$ and $U(t)$ on both side of the above equation and leaving $\frac{d\rho(t)}{dt}$ alone the left-hand side of the equation, one can obtain the following equation in the Shrödinger frame:

$$\frac{d\rho(t)}{dt} = -\frac{i}{\hbar}[H_0(t), \rho(t)] + 2\kappa(\sigma_z\rho(t)\sigma_z - \rho(t)). \tag{3.20}$$

Hence equation (3.20) shows the master equation averaged over Gaussian noise, in which the first term is the unitary dynamics, while the second one refers to the dissipation terms which is responsible for losing the energy out of the system.

3.2 Driven Two-Level System: Telegraph Noise

We study here the effect of random telegraph noise only on the two-level system whose Hamiltonian is given by

$$H = \frac{\hbar\,\epsilon}{2}\sigma_z + \frac{\hbar\,\Delta(t)}{2}\sigma_x, \tag{3.21}$$

where $\Delta(t)$ is the fluctuating tunneling term of TLS, and has a form: $\Delta_0 + \Delta_1\eta(t)$. Here Δ_0 is the static tunneling rate, while the Δ_1 is the amplitude of the noise that affects the tunneling rate. $\eta(t)$ is the random telegraph noise which is discussed in a detailed in section (2.2).

In order to solve dynamics of such a system, it is customary to use von-Neumann equation (2.2). Here it would be convenient to write the evolution density matrix in the Bloch vector (see the section (2.1)). It is worth noting that we can either use an ensemble averaging approach to achieve the noise averaged equations by solving equations (3.22-3.24) for a convenient number of different realizations of RTN noise and averaging solutions, or use the probability density of the RTN signal to average the coupled differential equations and solve those averaged equations. However, since the system contains a dichotomous process, one can utilize two theorems to solve analytically such a model. These are Bourret-Frisch [63] and Loginov-Shapiro [62] theorems. The former theorem allows us to factorize the multi-time correlation functions of the dichotomous signal, while second provides the average of the time-evolution operators of the noise with that of the system operators. Based on the above procedure, one can obtain the master equation and its Bloch vector expressions in the following way:

$$\begin{aligned}
\frac{d\rho}{dt} &= -\frac{i}{\hbar}\left[\begin{pmatrix} \hbar\,\epsilon/2 & \hbar\,\Delta(t)/2 \\ \hbar\,\Delta(t)/2 & -\hbar\,\epsilon/2 \end{pmatrix}, \begin{pmatrix} \rho_{11} & \rho_{12} \\ \rho_{21} & \rho_{22} \end{pmatrix}\right] \\
&= \begin{pmatrix} i\,\Delta(t)(\rho_{21}-\rho_{12})/2 & i\,\Delta(t)(\rho_{11}-\rho_{22})/2 - i\,\epsilon\,\rho_{12}/2 \\ -i\,\Delta(t)(\rho_{11}-\rho_{22})/2 + i\,\epsilon\,\rho_{21}/2 & -i\,\Delta(t)(\rho_{12}-\rho_{21})/2 \end{pmatrix}.
\end{aligned}$$

Above equation can be written in the Bloch vector form (see the section (2.1)):

$$\begin{aligned}
\dot{P}_x(t) &= -\epsilon\,P_y(t), && (3.22) \\
\dot{P}_y(t) &= \epsilon\,P_x(t) - \Delta(t)\,P_z(t), && (3.23) \\
\dot{P}_z(t) &= \Delta(t)\,P_y(t). && (3.24)
\end{aligned}$$

Equations (3.22)-(3.24) indicate the set of first order coupled differential equations that include the time dependent noisy term $\Delta(t)$. Let us first state the description of the Loginov-Shapiro theorem [62]:

$$\frac{d}{dt}\langle\eta(t)P_i(t)\rangle = -2\,\nu\langle\eta(t)P_i(t)\rangle + \langle\eta(t)\frac{d}{dt}P_i(t)\rangle \qquad (3.25)$$

where $\langle\ldots\rangle$ refers the averaged over RTN signal. $P_i(t)$ are the system operators: $P_{x,y,z}(t)$ and the terms $\langle\eta(t)P_i(t)\rangle$ are the noise correlator operator which might illustrate how much correlated the noise and the system operators are. We should note that the average of the above equation family can be obtained analytically by using two theorem we present above. By using the theorem, averaging over the noise $\Delta(t)$ in equations (3.22)-(3.24) would make the coupled differential equations doubled and as follows:

$$\begin{aligned}
\frac{d}{dt}\langle P_x(t)\rangle &= -\epsilon\,\langle P_y(t)\rangle, && (3.26)\\
\frac{d}{dt}\langle P_y(t)\rangle &= \langle \epsilon\, P_x(t) - (\Delta_0 + \Delta_1 \eta(t) P_z(t)\rangle \\
&= \epsilon\langle P_x(t)\rangle - \Delta_0\langle P_z(t)\rangle - \Delta_1\langle \eta(t) P_z(t)\rangle, && (3.27)\\
\frac{d}{dt}\langle P_z(t)\rangle &= \langle \Delta_0 + \Delta_1 \eta(t) P_y(t)\rangle \\
&= \Delta_0\langle P_y(t)\rangle + \Delta_1\langle \eta(t) P_y(t)\rangle, && (3.28)\\
\frac{d}{dt}\langle\, \eta(t) P_x(t)\rangle &= -2\nu\langle \eta(t) P_x(t)\rangle + \langle \eta(t)\, \underbrace{\frac{d}{dt} P_x(t)}_{\downarrow}\rangle \\
&= -2\nu\langle \eta(t) P_x(t)\rangle + \langle \eta(t)\, \overbrace{(-\epsilon P_y(t))}\rangle \\
&= -2\nu\langle \eta(t) P_x(t)\rangle - \epsilon\langle \eta(t) P_y(t)\rangle, && (3.29)\\
\frac{d}{dt}\langle \eta(t) P_y(t)\rangle &= -2\nu\langle \eta(t) P_y(t)\rangle + \langle \eta(t)\, \underbrace{\frac{d}{dt} P_y(t)}_{\downarrow}\rangle \\
&= -2\nu\langle \eta(t) P_y(t)\rangle + \langle \eta(t)\, \overbrace{(\epsilon\, P_x(t) - \Delta(t)\, P_z(t))}\rangle \\
&= -2\nu\langle \eta(t) P_y(t)\rangle + \langle \eta(t)(\epsilon P_x(t) - (\Delta_0 + \Delta_1 \eta(t)) P_z(t)\rangle \\
&= -2\nu\langle \eta(t) P_y(t)\rangle + \epsilon\langle \eta(t) P_x(t)\rangle - \Delta_0\langle \eta P_z(t)\rangle - \Delta_1\langle \eta(t)\eta(t) P_z(t)\rangle \\
&= -2\nu\langle \eta(t) P_y(t)\rangle + \epsilon\langle \eta(t) P_x(t)\rangle - \Delta_0\langle \eta P_z(t)\rangle - \Delta_1\langle P_z(t)\rangle, && (3.30)\\
\frac{d}{dt}\langle \eta(t) P_z(t)\rangle &= -2\nu\langle \eta(t) P_z(t)\rangle + \langle \eta(t)\, \underbrace{\frac{d}{dt} P_z(t)}_{\downarrow}\rangle \\
&= -2\nu\langle \eta(t) P_z(t)\rangle + \langle \eta(t)\, \overbrace{(\Delta(t) P_y(t))}\rangle \\
&= -2\nu\langle \eta(t) P_z(t)\rangle + \langle \eta(t)(\Delta_0 + \Delta_1 \eta(t)) P_y(t)\rangle \\
&= -2\nu\langle \eta(t) P_z(t)\rangle + \Delta_0\langle \eta P_y(t)\rangle + \Delta_1\langle \eta(t)\eta(t) P_y(t)\rangle \\
&= -2\nu\langle \eta(t) P_z(t)\rangle + \Delta_0\langle \eta P_y(t)\rangle + \Delta_1\langle P_y(t)\rangle. && (3.31)
\end{aligned}$$

Here, we obtain a set of six coupled differential equations for the population difference and the coherence of the TLS averaged over the RTN noise and the product of these quantities and the noise, again averaged over the same noise, namely $\langle \eta(t)\, P_{x,y,z}(t)\rangle$. Note that this doubling of the number of differential equations is one of the distinguishing properties of the Bourret-Frisch and Loginov-Shapiro theorems applied to system of differential equations that contain random telegraph noise terms. The existence of terms of the form $\langle \eta(t)\, P_{x,y,z}(t) \rangle$ is due to the fact that RTN is not Gaussian. From equations (3.26)-(3.28), one can see that $P_y(t)$ coherence connects the population difference $P_z(t)$ and coherence $P_x(t)$ in the absence of external noise which means that the systems exhibits non-zero $P_x(t)$ and $P_y(t)$ whenever the initial population difference is nonzero and/or y coherence is initially nonzero. The effect of noise is to enhance the connection between the population difference and y coherence through the terms $\langle \eta(t)\, P_{y,z}(t) \rangle$.

3.3 Driven Two-Level System: Gaussian and Telegraph Noise

In this section, we consider the combined effect of two external noises on the dynamics of the TLS. The Hamiltonian of the system with Gaussian noise disturbing energy levels and transition rate fluctuations as random telegraph noise is given by

$$H = \frac{\hbar\epsilon}{2}\sigma_z - \frac{\hbar\Delta(t)}{2}\sigma_x + \frac{\hbar\epsilon(t)}{2}\sigma_z. \tag{3.32}$$

Here we use two different independent noises that influence the static parameters, namely the transition energy and the coupling constants, of the tunneling model. We have presented a review of the noises–$\epsilon(t)$ and $\Delta(t)$–in section (3.1) for Gaussian and section (3.2) for telegraph noise, respectively. In order to solve such a system one attempt is to first isolate the effect of the Gaussian noise $\epsilon(t)$, and to transform H in equation (3.32) into the interaction picture by utilizing the unitary evolution operator $U(t)$ in equation (3.2), which results in employing the average over the ϵ term and obtaining the Liouville-von

Neumann equation we already obtained in section (3.1):

$$\frac{d\langle\rho\rangle}{dt} = -\frac{i}{\hbar}[H_0(t), \langle\rho\rangle] + 2\kappa(\sigma_z\langle\rho\rangle\sigma_z - \langle\rho\rangle), \tag{3.33}$$

Where $\langle\ldots\rangle$ represents the averaging process over the $\epsilon(t)$ term. Here, the Hamiltonian consists of static and time-dependent RTN noise terms: $H_0(t) = \hbar\,\epsilon\sigma_z/2 - \hbar\Delta(t)\sigma_x/2$.

Since the master equation in equation (3.33) includes another external noise, i.e., RTN signal, we use the Loginov-Shapiro theorem [62] in the Bloch vector representation of the density matrix. One can obtain the first-order coupled differential equation:

$$\begin{aligned}
\frac{d}{dt}\langle P_x(t)\rangle &= -4\kappa\langle P_x(t)\rangle - \epsilon\langle P_y(t)\rangle, && (3.34)\\
\frac{d}{dt}\langle P_y(t)\rangle &= \epsilon\langle P_x(t)\rangle - 4\kappa\langle P_y(t)\rangle + (\Delta_0 + \Delta_1\eta(t))\langle P_z(t)\rangle, && (3.35)\\
\frac{d}{dt}\langle P_z(t)\rangle &= -(\Delta_0 + \Delta_1\eta(t))\langle P_y(t)\rangle. && (3.36)
\end{aligned}$$

According to Loginov-Shapiro theorem [62] (see equation (3.25)) one can find the set of six first-order coupled differential equations by using the findings of equations (3.34)-(3.36) as follows:

$$\begin{aligned}
\frac{d}{dt}\langle\langle P_x(t)\rangle\rangle &= -4\kappa\langle\langle P_x(t)\rangle\rangle - \epsilon\langle\langle P_y(t)\rangle\rangle, && (3.37)\\
\frac{d}{dt}\langle\langle P_y(t)\rangle\rangle &= \epsilon\langle\langle P_x(t)\rangle\rangle - 4\kappa\langle\langle P_y(t)\rangle\rangle + \Delta_0\langle\langle P_z(t)\rangle\rangle \\
&+ \Delta_1\langle\langle\eta(t)P_z(t)\rangle\rangle, && (3.38)\\
\frac{d}{dt}\langle\langle P_z(t)\rangle\rangle &= -\Delta_0\langle\langle P_y(t)\rangle\rangle - \Delta_1\langle\langle\eta(t)P_y(t)\rangle\rangle. && (3.39)
\end{aligned}$$

Note that $\langle\langle\ldots\rangle\rangle$ stands for the average equations over both noises. Since above equations (3.38)-(3.39) contain noise correlator terms–$\langle\langle\eta(t)P_{y,z}(t)\rangle\rangle$– one should compute the average of correlators $\langle\eta(t)P_i(t)\rangle$ with $i = x, y, z$ by using the relation in equation (3.25):

$$\begin{aligned}
\frac{d}{dt}\langle\langle\eta(t)P_x(t)\rangle\rangle &= -2\nu\langle\langle\eta(t)P_x(t)\rangle\rangle + \langle\langle\eta(t)\underbrace{\frac{d}{dt}P_x(t)}_{\downarrow}\rangle\rangle, \\
&= -2\nu\langle\langle\eta(t)P_x(t)\rangle\rangle + \langle\langle\eta(t)\overbrace{(-4\kappa P_x(t) - \epsilon P_y(t))}\rangle\rangle, \\
&= -2\nu\langle\langle\eta(t)P_x(t)\rangle\rangle - 4\kappa\langle\langle\eta(t)P_x(t)\rangle\rangle \\
&\quad -\epsilon\langle\langle\eta(t)P_y(t)\rangle\rangle, \qquad (3.40) \\
\frac{d}{dt}\langle\langle\eta(t)P_y(t)\rangle\rangle &= -2\nu\langle\langle\eta(t)P_y(t)\rangle\rangle + \langle\langle\eta(t)\underbrace{\frac{d}{dt}P_y(t)}_{\downarrow}\rangle\rangle, \\
&= \langle\langle\eta(t)\overbrace{(\epsilon P_x(t) - 4\kappa P_y(t) + (\Delta_0 + \Delta_1\eta(t))P_z(t))}\rangle\rangle \\
&\quad -2\nu\langle\langle\eta(t)P_y(t)\rangle\rangle, \\
&= -2\nu\langle\langle\eta(t)P_x(t)\rangle\rangle - (2\nu + 4\kappa)\langle\langle\eta(t)P_y(t)\rangle\rangle \\
&\quad +\Delta_0\langle\langle\eta(t)P_z(t)\rangle\rangle + \Delta_1\underbrace{\langle\langle\eta(t)\eta(t)P_z(t)\rangle\rangle}_{\langle\langle P_z(t)\rangle\rangle}, \qquad (3.41)
\end{aligned}$$

where the last term of equation (3.41) would be $\Delta_1\langle\langle P_z(t)\rangle\rangle$ due to the remarkable property of the dichotomous Markov process i.e., $\eta(t)^2 = 1$ [61]. The rest of the equations can be obtained by using the above procedure:

$$\begin{aligned}
\frac{d}{dt}\langle\langle\eta(t)P_z(t)\rangle\rangle &= -2\nu\langle\langle\eta(t)P_z(t)\rangle\rangle + \langle\langle\eta(t)\underbrace{\frac{d}{dt}P_z(t)}_{\downarrow}\rangle\rangle, \\
&= -2\nu\langle\langle\eta(t)P_z(t)\rangle\rangle - \langle\langle\eta(t)\overbrace{(\Delta_0 + \Delta_1\eta(t))P_y(t))}\rangle\rangle, \\
&= -2\nu\langle\langle\eta(t)P_z(t)\rangle\rangle - \Delta_0\langle\langle\eta(t)P_y(t)\rangle\rangle \\
&\quad -\Delta_1\langle\langle P_y(t)\rangle\rangle. \qquad (3.42)
\end{aligned}$$

One can write the set of equations (3.37)-(3.42) in the column vector form as functions of the averaged system parameters $\langle\langle P_i(t)\rangle\rangle$ and the noise correlators $\langle\langle\eta(t)P_i(t)\rangle\rangle$:

$$\frac{d\overrightarrow{Y}}{dt} = M\overrightarrow{Y}. \qquad (3.43)$$

Here

$$\overrightarrow{Y} = \begin{bmatrix} \langle\langle P_x(t)\rangle\rangle \\ \langle\langle P_y(t)\rangle\rangle \\ \langle\langle P_z(t)\rangle\rangle \\ \langle\langle \eta(t)P_x(t)\rangle\rangle \\ \langle\langle \eta(t)P_y(t)\rangle\rangle \\ \langle\langle \eta(t)P_z(t)\rangle\rangle \end{bmatrix} \text{ and } M = \begin{bmatrix} -4\kappa & -\epsilon & 0 & 0 & 0 & 0 \\ \epsilon & -4\kappa & \Delta_0 & 0 & 0 & \Delta_1 \\ 0 & -\Delta_0 & 0 & 0 & -\Delta_1 & 0 \\ 0 & 0 & 0 & -2\nu-4\kappa & -\epsilon & 0 \\ 0 & 0 & \Delta_1 & \epsilon & -2\nu-4\kappa & \Delta_0 \\ 0 & -\Delta_1 & 0 & 0 & -\Delta_0 & -2\nu \end{bmatrix}$$

It is important to note that the solution in equation (3.43) is exact and completely describes the dynamics of the system.

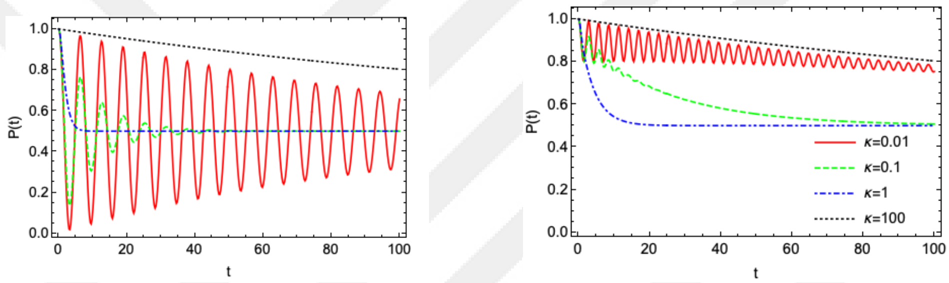

(a) $\epsilon = 0$ (b) $\epsilon = 2$

Figure 3.1: The dynamics of the population at four different κ values which are 0.01, 0.1, 1.0 and 100 (a) $\epsilon = 0$ (b) $\epsilon = 2$ with the other parameters: $\Delta_0 = 1$, $\Delta_1 = 0$ and $\nu = 0$.

We will present and discuss the solutions to equation (3.43) for a number of representative parameters set below. First, we start with a system that has only Gaussian noise and present the population–$P(t) = (1 + \langle\langle P_z(t)\rangle\rangle)/2$– dynamics for four distinct values of the noise strength κ for the biased and biased cases. The expectation is that as κ is increased, the population will approach the stationary value of 1/2 faster. Figure 3.1(a) indicates that the expectation is satisfied until a specific value of κ (=1 in the graph), but further increase in κ causes the system to transition to a different dynamical regime which is an exponential decay with much smaller decay constant. A further increase in κ might even cancel the whole tunneling dynamics. Figure 3.1(b) shows that biased and unbiased dynamics are qualitatively similar except that $P(t)$ at the lowest κ display damped oscillatory dynamics centered around not 1/2 but a decreasing value.

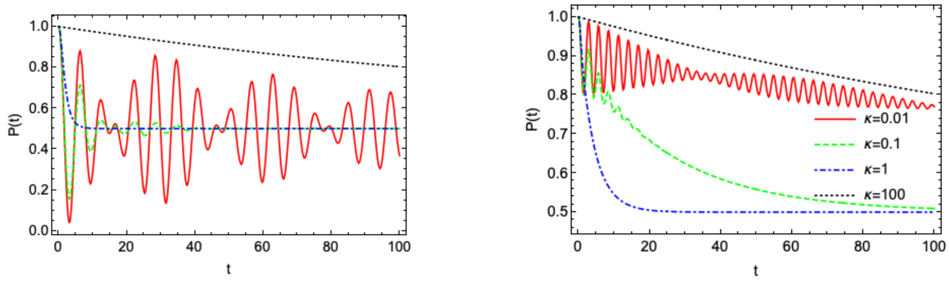

(a)$\epsilon = 0$ (b) $\epsilon = 2$

Figure 3.2: Same as figure 3.1 except the noise amplitude $\Delta_1 = 0.1$.

Figure 3.2(a)-(b) displays the population dynamics of the system driven by both noises $\epsilon(t)$ and $\Delta(t)$ for unbiased and biased, respectively. Noise frequency is in the limit case $\nu = 0$, which causes the superposition of the two solutions with two static tunneling matrix terms $\Delta_{\pm} = \Delta_0 \pm \Delta_1$. Figure 3.2(a) with unbiased case illustrates that the dynamics of $P(t)$ has a richer behavior than the finding of figure 3.1, which is called a beating phenomenon [5]. For the biased case, one can observe the same phenomenon in a much smaller decay constant. At the low value of κ $(= 0.01)$, such a tendency is prominent irrespective of the value of ϵ in figure 3.2(a)-(b), while further increasing κ dominates the oscillations, which results in observing exponentially decaying.

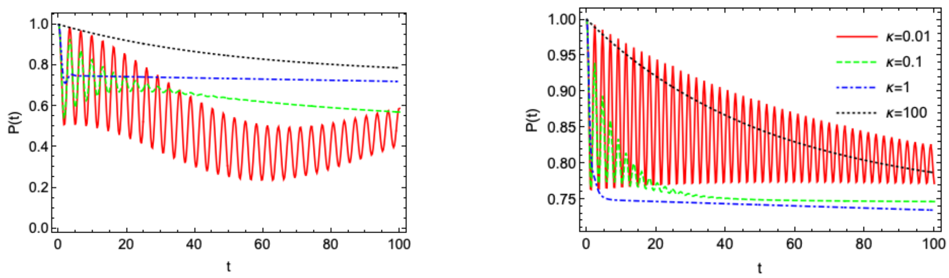

(a)$\epsilon = 0$ (b)$\epsilon = 2$

Figure 3.3: Same as the figure 3.2 except the noise amplitude $\Delta_1 = 0.95$.

We also plot the graph of the dynamics $P(t)$ at high noise amplitude $\Delta =$

0.95 in figure 3.3 compared to that of figure 3.2. The most important finding is that when $\Delta_1 \approx \Delta_0$, which means Δ_- is much different than Δ_+, it is found to be more like a localization phenomenon in a potential double well, namely the system tends to stay one of the wells having only fast oscillations in it (see figure 3.3(a)). For the biased case ($\epsilon \neq 0$) one can observe that $P(t \approx \infty) > 1/2$.

RESULT AND DISCUSSIONS

In this chapter, we present and discuss the main findings of the thesis on the effect of two different noises on three quantum measures: namely, quantum coherence, relative entropy, and non-Markovianity measures. These results are presented in two sections: static and fluctuating barriers (see Ref.[70]).

Since we analyze the tunneling problem, there should always be a constant tunneling rate between two wells, that is, $\Delta_0 = 1$. The remaining parameters are free to choose which are scaled with respect to Δ_0 and presented in dimensionless units ($\hbar = k_B = 1$). In the following, we will investigate the barrier and its random disturbance on the coherence dynamics and non-Markovianity for the unbiased ($\epsilon = 0$) and biased ($\epsilon = 2.0$) cases. Since we neglect any quantum features of the environment leading to stochastic energy bias, we consider that it always exists but plays a secondary role, so we fixed $\kappa = 0.1$ in our calculations.

4.1 Static Barrier

In the first analyzed case, we assume that the barrier is static (that is, $\Delta_1 = 0$). The dynamic equations presented in equation (3.43) can be solved analytically. For the unbiased case ($\epsilon = 0$) and the initial states considered $\rho_1(0)$ and $\rho_2(0)$, the l_1 norm of coherence takes simple forms.

$$\begin{aligned} C_{l_1}(\rho_1(0)) &= \left| \frac{e^{-\kappa t} \sin(\Omega t)}{\Omega} \right|, \\ C_{l_1}(\rho_2(0)) &= \left| e^{-\kappa t} \frac{\Delta_0}{\Omega} \cos(t\,\Omega + \theta) \right|, \end{aligned} \tag{4.1}$$

Where $\Omega = \sqrt{\Delta_0^2 - \kappa^2}$ and $\theta = \arctan(\kappa/\Omega)$. It is obvious from equation (4.1) that l_1 norm of coherence exhibits damped oscillations. However, for the biased case, the analytical equations are too long and uninspiring. Therefore, in figure 4.1, we plot the dynamics of coherence for the biased and unbiased cases and the initial states $\rho_1(0)$ (figure 4.1(a)) and $\rho_2(0)$ (figure 4.1(b)). To elucidate the influence of the barrier on coherence dynamics, we first consider the case where there is no barrier (that is, $\Delta_0 = 0$). In this scenario, there is only bias and its damping induced by its coupling to the high-temperature thermal environment. Therefore, $C_{l_1}(\rho)$ simply decays exponentially in time for the initial coherent state $\rho_2(0)$, while it always stays zero for the initial incoherent one $\rho_1(0)$ (see also equation (4.1)). Introducing a barrier, on the other hand, substantially changes the coherence dynamics. As shown in figure 4.1(a), coherence is induced in the initial incoherent state $\rho_1(0)$. For both initial states, $C_{l_1}(\rho)$ shows damp oscillatory behavior. The damping is raised by its coupling to the thermal environment where the parameter κ just controls how fast the coherence decays. In figure 4.1, unbiased ($\epsilon = 0$) and biased ($\epsilon = 2$) cases are also presented. It is clear from the figure that ϵ decreases the amplitude of oscillations. Note that, non-zero bias makes tunneling more difficult, since it introduces a gap between two localized potential wells [5]. On the other hand, as shown by the comparison of figure 4.1(a) with figure 4.1(b), the coherence dynamics exhibit adverse behavior for the two initial states. Even though the induced coherence (figure 4.1(a)) is more robust to dissipation for the biased case (green dashed line) compared to the unbiased one (red solid line), the behavior is reversed for the initial coherent state (figure 4.1(b)).

We should emphasis that for the static barrier case, the Gaussian noise $\epsilon(t)$ modeled as the delta correlated function acts only as the source of the environment. Such noise can mimic the interaction of a system with quantum oscillators of a reservoir in the high temperature limit [59]. Under the approximation, the environment would be classical, and there would be no back-flow of information from the environment to the system. After a straightforward calculation, the non-Markovianity measure in equation (2.12) for the initially orthogonal pair states $\rho_1(0)$ and $\rho_3(0)$ is found to be exactly zero. The re-

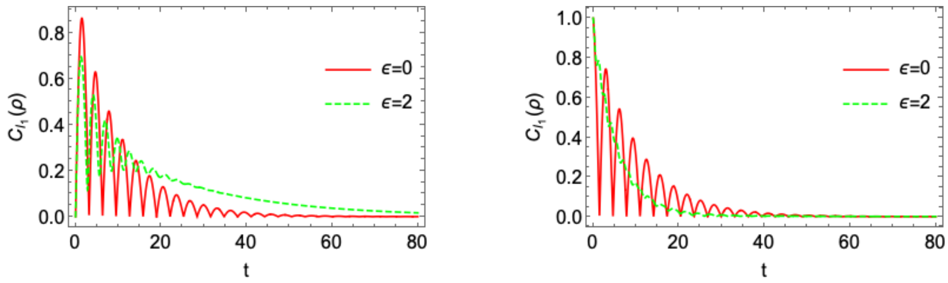

(a) Initial state: $\rho_1(0)$ (b) Initial state: $\rho_2(0)$

Figure 4.1: l_1 norm of coherence $C_{l_1}(\rho)$ is plotted as a function of time t for the static barrier case ($\Delta_1 = 0$) and the parameters $\Delta_0 = 1$, $\kappa = 0.1$, $\epsilon = 0$ (red, solid line) and $\epsilon = 2.0$ (green, dashed line). (a) is plotted for the initially non-coherent state $\rho_1(0)$, while (b) is for the initially coherent one $\rho_2(0)$.

sult can also be interpreted from the master equation (3.33) which is obtained after averaging over Gaussian noise $\epsilon(t)$. The master equation is in the Lindblad form and can always be represented by a completely positive and trace-preserving map [46]. The distinguishability is therefore reduced monotonically during the dynamical evolution. The only effect of κ is to increase dissipation which may reduce the amplitude of oscillations and to speed up the decay.

4.2 Fluctuating Barrier

We next investigate the role of the barrier fluctuations on quantum coherence and elucidate its non-Markovian character. There are two parameters that characterize the fluctuations in the barrier. One of them is Δ_1 which gives the amplitude of the noise. The other one is ν, which determines the fluctuation frequency. Instead of focusing on these parameters separately, we will consider the ratio known as the Kubo number $K = \Delta_1/\nu$ [8]. It is a proper measure of the color of the noise. For example, when the amplitude Δ_1 is fixed, $K \ll 1$ indicates a weakly colored noise due to the very fast barrier fluctuations, while $K \gg 1$ dictates strongly colored (slow) noise. In the case of $K \ll 1$, the system barely feels the effect of noise. In this scenario, the barrier can be considered to be almost static and the results presented in the previous sections are the same. On the other hand, in the case where $K \gg 1$

the system dynamics is governed by the superposition of two solutions with tunneling rates $\Delta_0 + \Delta_1$ and $\Delta_0 - \Delta_1$.

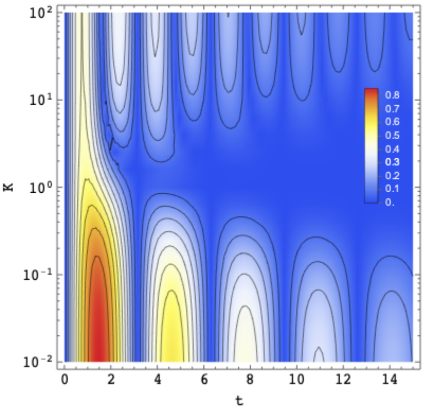

(a) $\epsilon = 0$

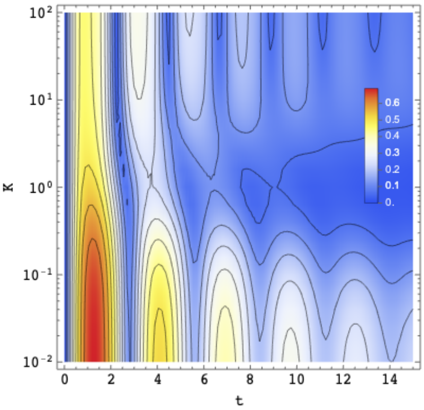

(b) $\epsilon = 2$

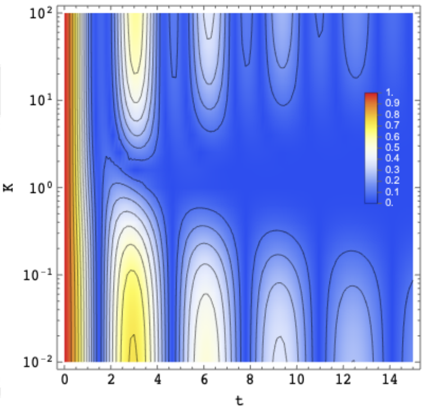

(c) $\epsilon = 0$

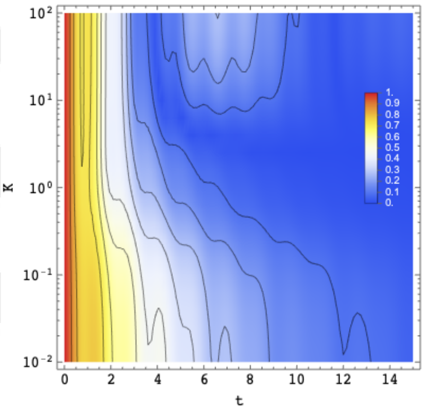

(d) $\epsilon = 2$

Figure 4.2: Contour plot of $C_{l_1}(\rho)$ as a function of dimensionless time and Kubo number $K = \Delta_1/\nu$ for the parameters $\Delta_0 = \Delta_1 = 1.0$, $\kappa = 0.1$, $\epsilon = 0$ ((a) and (c)) and $\epsilon = 2.0$ ((b) and (d)). While the sub-figures (a) and (b) are plotted for the initial incoherent state $\rho_1(0)$, (c) and (d) are for the initial coherent state $\rho_2(0)$. In the plots 10 equidistant contour lines are considered between zero and the maximum value.

For the fluctuating barrier case, it is not possible to obtain a simple analytical expression for the coherence measure. Therefore, we only analyze the results numerically. In figure 4.2, we present contour plots of the l_1 norm of coherence as a function of the Kubo number K and the dimensionless time for the initial coherent and incoherent states. Both unbiased and biased cases are considered. The general observation from figure 4.2 is that the $C_{l_1}(\rho)$ displays a damped oscillating time dependence irrespective of the properties of the RTN noise. This finding can be accounted for by noting that both the thermal dephasing noise and RTN on the barrier height lead to the destruction of the coherence in the long time limit. For the initial incoherent state $\rho_1(0)$ (figure 4.2(a) and figure 4.2(b)), the maximum coherence is observed in regions where Kubo number $K \ll 1$ corresponds to weakly colored noise. However, there is an exceptional region where $C_{l_1}(\rho)$ is independent of the value of K in a very short time limit for the coherent initial state $\rho_2(0)$ (see figure 4.2(c) and figure 4.2(d)). It can also be seen from figure 4.2 that the boundary $K \approx 1$ divides the dynamics of coherence into two different regimes with respect to the noise color, i.e., in the limit of $K \to 1$ (intermediate colored noise), coherence decays exponentially, while for weak and strong colored noise, one can observe a strong death-rebirth cycle for coherence with the damping rate ν for all sub-figures of figure 4.2. Regardless of the value of ϵ and the initial state, the decoherence lifetime strongly depends on the Kubo number and has a resonance-like behavior that decreases with increasing K until the critical value $K = 1$ and then tends to increase.

Finally, we discuss the non-Markovian effects of random barrier fluctuations on quantum coherence. In this sense, we present some analytical results for the non-Markovianity measure (equation (2.12)) when only RTN parameters are non-zero (i.e., $\epsilon = \kappa = \Delta_0 = 0$). Here, we are able to show the non-Markovian property of barrier fluctuations. By solving the dynamical equations in equation (3.43) for the initial states $\rho_1(0)$ and $\rho_3(0)$, one can easily obtain the distinguish-ability as

$$\Delta_{tr}(\rho_1, \rho_3) = \left| \frac{e^{-\nu t}}{\gamma} \left(\gamma \cos(\gamma t) + \nu \sin(\gamma t)\right) \right|. \tag{4.2}$$

The trace distance exhibits damped oscillating behavior with noise frequency ν and $\gamma = -\sqrt{\Delta_1 - \nu}$. Note that, when $\nu > \Delta_1$, γ is purely imaginary, so $\Delta_{tr}(\rho_1, \rho_3)$ is a uniformly decreasing function of time, so $\mathcal{N} = 0$. Using $\sigma(\rho_1, \rho_3)$ of equation (4.2) and the non-Markovianity in equation (2.12), $\mathcal{N}$ for

$\Delta_1 > \nu$ can be obtained as follows:

$$\mathcal{N} = \frac{1}{-1 + e^{\frac{\pi}{\sqrt{K^2-1}}}}. \tag{4.3}$$

The obtained expression $\mathcal{N}$ strongly depends on the square of the noise color K. One can note that when $K \ll 1$ (almost static barrier), $\mathcal{N} = 0$. For a more general case, it is not possible to give an analytical expression for non-Markovianity. Instead, for the general case, we display the results of numerical solutions in figure 4.3 as the contour lines of $\mathcal{N}$ as the functions of the Kubo number K and the thermal noise strength κ for the system including both the thermal and external noise for the unbiased (figure 4.3(a)) and biased (figure 4.3(b)) cases. The most prominent observation from figure 4.3 is that $\mathcal{N}$ increases with increasing K and with decreasing κ for unbiased and biased cases. Ref. [68] has been found that $\mathcal{N}$ increases with increasing Kubo number for the non-equilibrium dephasing model. It is obvious from figure 4.3 that the system dynamics is Markovian at high κs. It can also be deduced from figure 4.3(a) (figure 4.3(b)) that Markovian-non-Markovian transition is (not) abrupt at $K = 1$ line for unbiased (biased) case. This transition is also reported for a pure dephasing model with non-equilibrium noise by Cai and Zeng [71]. At the limit $K \to 0$, RTN approaches the white-noise [8], which can create only Markovian dynamics. Therefore, as expected, we find that the dynamics are also Markovian in this parameter regime (see figure 4.3). On the other hand, the time dependence of coherence displays an opposite trend to the noise color. For small K, the decoherence time is longer for both initially coherent and incoherent states (see figure 4.2), which can be understood by examining the low and high-frequency limits of RTN.

One of the general insights from the above findings is that the decoherence time does not show a monotonous trend with respect to the Kubo number. That is, it decreases with increasing K until $K = 1$, and then starts to increase with increasing K for initially coherent and non-coherent states in both unbiased and biased cases (see figure 4.2). $K = 1$ seems to play an essential role in both the existence of non-Markovianity and decoherence time. The noise color dependence of the decoherence rate displays a resonance structure with a peak at $K = 1$ if decoherence rate is defined as the inverse of decoherence time. Also, at $K = 1$ the coherence decays exponentially without any oscillations (see figure 4.2(a-d)). Hence, although there is no direct relation between coherence and non-Markovianity, both properties have special structures around $K = 1$.

In some studies of the coherence-Markovianity relation, authors report a direct connection between those two quantities for the model systems they investigate. For example, Ref.[54] found that the stationary coherence is maximized for non-Markovian dynamics in an Ohmic spin-boson model at low temperatures. As we study the effect of classical noise which is an infinite temperature limit, the stationary value of coherence is zero. But, figure 4.2 and figure 4.3 indicate that one can observe the decoherence rate is higher when the dynamics is non-Markovian, which seems to contradict the findings reported in Ref. [48, 53, 54, 55]. Ref.[55] studied a global system–bath interaction in the both absence and presence of non-Markovian noise. Also, our findings are in contrast with those reported in Ref. [53] which studied a collisional model where both the system and environment are composed of spin-1/2 particles and found that the higher non-Markovianity leads to a low decoherence rate. On the other hand, Chanda and Bhattacharya [52] analyzed the dephasing channel and found similar coherence-non-Markovianity relation to our results. Hence, our findings apparently indicate that the connection between non-Markovianity and decoherence is system-dependent and is not universal.

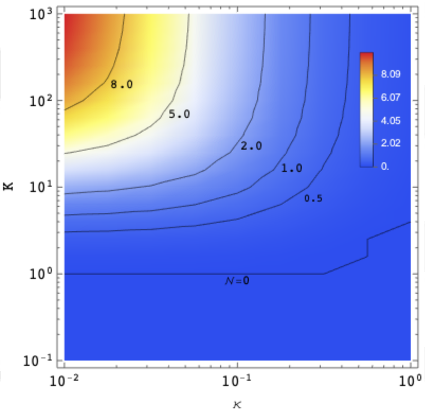

(a) $\epsilon = 0$

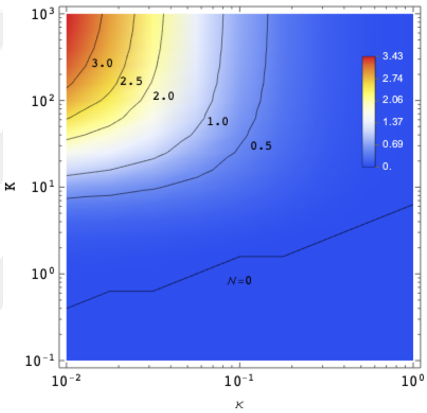

(b) $\epsilon = 2$

Figure 4.3: Non-Markovianity $\mathcal{N}$ is plotted as functions of κ and Kubo number $K = \Delta_1/\nu$ for the parameters $\Delta_0 = \Delta_1 = 1.0$, $\epsilon = 0$ (a) and $\epsilon = 2.0$ (b). 6 contour lines are chosen between the minimum and maximum values of $\mathcal{N}$. Note that, $\mathcal{N}$ is computed for $\rho_1(0)$ and $\rho_3(0)$.

CONCLUSIONS AND RECOMMENDATIONS

In this thesis, we have reported the results of an in-depth study of the effect of noise on the quantum tunneling system in which there exist stochastic bias and a fluctuating barrier under the two-level approximation. The main goal of this thesis was to examine the dependence of quantum coherence dynamics on the correlation time of the barrier fluctuations and to explain their non-Markovian nature. The prominent findings of the thesis on the influence of two distinct noises on three quantum measures–quantum coherence, relative entropy, and non-Markovianity–are presented in chapter 3 and discussed in chapter 4 in a way of two distinct sections: static and fluctuating barriers. We have obtained the analytical solutions for coherence measure–$C_{l_1}(\rho)$–and non-Markovianity–$\mathcal{N}$–for non-coherent and completely coherent beginning states for a constrained range of system and noise parameters, which is the one of the main findings of the thesis. The dynamics of the system are determined to be non-Markovian only when the RTN barrier fluctuations fulfill $K \gg 1$, which means that the noise amplitude is greater than the noise frequency. We have discovered that there is no direct relationship between system coherence and non-Markovianity of system dynamics, except that both $\mathcal{N}$ and $C_{l_1}(\rho)$ change character around $K = 1$. However, for both biased and non-biased two-level systems, a consistent relationship between the decoherence rate and non-Markovianity could be demonstrated for all of the distinct initial states. Surprisingly, we have shown that the decoherence rate of non-Markovian dynamics is greater than that of Markovian dynamics. Because the non-Markovianity we utilized is dependent on information flow from the environment to the system, one would anticipate coherence to decay slower in such a setting, as observed for a number of systems [48, 53, 54, 55].

We hope the main findings of the current thesis might contribute to the development of quantum computer technologies. All of these technologies rely on properties of quantum mechanics, such as quantum entanglement, quantum superposition, and quantum tunnelings, such as quantum cryptography, quantum simulation, quantum metrology, and quantum imaging.

REFERENCES

Vancouver citation system was used in this thesis.

1. Cohen-Tannoudji C, Diu B, Laloë F. Quantum Mechanics, Volume 3: Fermions, Bosons, Photons, Correlations, and Entanglement: John Wiley &Sons; 2019.

2. Trixler F. Quantum tunnelling to the origin and evolution of life. Curr. Org. Chem. 2013;17(16):1758-70.

3. Taylor JR, Zafiratos CD, Dubson MA. Modern physics for scientists and engineers; 2004.

4. Ionescu AM, Riel H. Tunnel field-effect transistors as energy-efficient electronic switches. Nature. 2011;479(7373):329-37.

5. Iwaniszewski J. Tunneling through a fluctuating barrier: Two-level model. Phys. Rev. E. 2000;61(5):4890.

6. Leggett A J, Chakravarty S, Dorsey A T, Fisher M P, Garg A, Zwerger W. Dynamics of the dissipative two-state system. Rev. Mod. Phys. 1987;59(1):1.

7. Weiss U, Quantum Dissipative Systems. Singapore; River Edge, NJ:World Scientific; 1993.

8. Goychuk I, Petrov E, May V. Dynamics of the dissipative two-level system driven by external telegraph noise. Phys. Rev. E. 1995;52(3):2392.

9. Cukier R. M. Morillo in Molecular Electronics. Blackwell Science; 1997.

10. Grifoni M, Hänggi P. Driven quantum tunneling. Phys. Rep. 1998;304(5-6):229-354.

11. Grifoni M. Dynamics of the dissipative two-state system under AC modulation of bias and coupling energy. Phys. Rev. E. 1996;54(4):R3086.

12. Grifoni M, Winterstetter M, Weiss U. Coherences and populations in the driven damped two-state system. Phys. Rev. E. 1997;56(1):334.

13. Goychuk I, Petrov E, May V. Bridge-assisted electron transfer driven by dichotomically fluctuating tunneling coupling. The J. Chem. Phys. 1995;103(12):4937-44.

14. Petrov E, Goychuk I, Teslenko V, May V. An exact solution of the stochastic Liouville equation: The two-level system coupled to an asymmetric dichotomous field. Phys. Lett. A. 1996;218(3-6):343-8.

15. Petrov E, Goychuk I, May V. Effective transfer rates for a dissipative two-level system driven by regular and stochastic fields. Phys. Rev. E. 1996;54(5):R4500.

16. Goychuk I, Petrov E, May V. Control of long-range electron transfer in dynamically disordered molecular systems by an external periodic field. J. Chem. Phys. 1997;106(11):4522-30.

17. Makri N, Sim E, Makarov DE, Topaler M. Long-time quantum simulation of the primary charge separation in bacterial photosynthesis. Proceedings of the National Academy of Sciences. 1996;93(9):3926-31.

18. Daizadeh I, Medvedev E S, Stuchebrukhov A A. Effect of protein dynamics on biological electron transfer. Proceedings of the National Academy of Sciences. 1997;94(8):3703-8.

19. Weisbuch C, Vinter B. Quantum semiconductor structures: fundamentals and applications: Elsevier; 2014.

20. Zhu Z-G, Su G, Zheng Q-R, Jin B. Time-dependent spin-polarized transport through a resonant tunneling structure with multiterminals. Phys. Rev. B. 2004;70(17):174403.

21. Daninthe H, Foteinopoulou S, Soukoulis C. Omni-reflectance and enhanced resonant tunneling from multilayers containing left-handed materials. Photonics and Nanostructures-Fundamentals and Applications. 2006;4(3):123-31.

22. Büttiker M, Landauer R. Traversal time for tunneling. Phys. Rev. Lett. 1982;49(23):1739.

23. Burmeister G, Maschke K. Scattering by time-periodic potentials in one dimension and its influence on electronic transport. Phys. Rev. B. 1998;57(20):13050.

24. Nielsen MA, Chuang IL. Quantum information and quantum computation. Cambridge: Cambridge University Press. 2000;2(8):23.

25. Lostaglio M, Korzekwa K, Jennings D, Rudolph T. Quantum coherence, time-translation symmetry, and thermodynamics. Phys. Rev. X. 2015;5(2):021001.

26. Plenio MB, Huelga SF. Dephasing-assisted transport: quantum networks and biomolecules. New J. Phys. 2008;10(11):113019.

27. Demkowicz-Dobrzański R, Maccone L. Using entanglement against noise in quantum metrology. Phys. Rev. Lett. 2014;113(25):250801.

28. Baumgratz T, Cramer M, Plenio MB. Quantifying coherence. Phys. Rev. Lett. 2014;113(14):140401.

29. Yu X-D, Zhang D-J, Xu G, Tong D. Alternative framework for quantifying coherence. Phys. Rev. A. 2016;94(6):060302.

30. Yu X-D, Zhang D-J, Liu C, Tong D. Measure-independent freezing of quantum coherence. Phys. Rev. A. 2016;93(6):060303.

31. Streltsov A, Singh U, Dhar HS, Bera MN, Adesso G. Measuring quantum coherence with entanglement. Phys. Rev. Lett. 2015;115(2):020403.

32. Yao Y, Xiao X, Ge L, Sun C. Quantum coherence in multipartite systems. Phys. Rev. A. 2015;92(2):022112.

33. Xi Z, Li Y, Fan H. Quantum coherence and correlations in quantum system. Sci. Rep. 2015;5(1):1-9.

34. Ma J, Yadin B, Girolami D, Vedral V, Gu M. Converting coherence to quantum correlations. Phys. Rev. Lett. 2016;116(16):160407.

35. Radhakrishnan C, Parthasarathy M, Jambulingam S, Byrnes T. Distribution of quantum coherence in multipartite systems. Phys. Rev. Lett. 2016;116(15):150504.

36. Winter A, Yang D. Operational resource theory of coherence. Phys. Rev. Lett. 2016;116(12):120404.

37. Bromley TR, Cianciaruso M, Adesso G. Frozen quantum coherence. Phys. Rev. Lett. 2015;114(21):210401.

38. Chitambar E, Streltsov A, Rana S, Bera M, Adesso G, Lewenstein M. Assisted distillation of quantum coherence. Phys. Rev. Lett. 2016;116(7):070402.

39. Ribeiro P, Vieira VR. Non-Markovian effects in electronic and spin transport. Phys. Rev. B. 2015;92(10):100302.

40. Abiuso P, Giovannetti V. Non-Markov enhancement of maximum power for quantum thermal machines. Phys. Rev. A. 2019;99(5):052106.

41. Pezzutto M, Paternostro M, Omar Y. An out-of-equilibrium non-Markovian quantum heat engine. Quantum Sci. Technol. 2019;4(2):025002.

42. Katz G, Kosloff R. Quantum thermodynamics in strong coupling: Heat transport and refrigeration. Entropy. 2016;18(5):186.

43. Ptaszyński, K. Non-Markovian thermal operations boosting the performance of quantum heat engines. Phys. Rev. E. 2022;106(1):014114.

44. Zhang X, Huang X, Yi X. Quantum Otto heat engine with a non-Markovian reservoir. J. Phys. A Math. Theor. 2014;47(45):455002.

45. Breuer H-P, Laine E-M, Piilo J. Measure for the degree of non-Markovian behavior of quantum processes in open systems. Phys. Rev. Lett. 2009;103(21):210401.

46. Laine E-M, Piilo J, Breuer H-P. Measure for the non-Markovianity of quantum processes. Phys. Rev. A. 2010;81(6):062115.

47. Kurt A. Two-time correlation functions beyond quantum regression theorem: effect of external noise. Quantum Inf. Process. 2021;20(7):1-17.

48. Radhakrishnan C, Chen P-W, Jambulingam S, Byrnes T, Ali M. Time dynamics of quantum coherence and monogamy in a non-Markovian environment. Sci. Rep. 2019;9(1):1-10.

49. Mirafzali S, Baghshahi H. Non-Markovianity detection with coherence measures based on the Tsallis relative entropies. Phys. A: Stat. Mech. Appl. 2019;514:274-9.

50. Man Z-X, Xia Y-J, Franco RL. Temperature effects on quantum non-Markovianity via collision models. Phys. Rev. A. 2018;97(6):062104.

51. He Z, Zeng H-S, Li Y, Wang Q, Yao C. Non-Markovianity measure based on the relative entropy of coherence in an extended space. Phys. Rev. A. 2017;96(2):022106.

52. Chanda T, Bhattacharya S. Delineating incoherent non-Markovian dynamics using quantum coherence. Ann. Phys. 2016;366:1-12.

53. Çakmak B, Pezzutto M, Paternostro M, Müstecaplıoğlu Ö. Non-Markovianity, coherence, and system-environment correlations in a long-range collision model. Phys. Rev. A. 2017;96(2):022109.

54. Addis C, Brebner G, Haikka P, Maniscalco S. Coherence trapping and information backflow in dephasing qubits. Physical Review A. 2014;89(2):024101.

55. Bhattacharya S, Banerjee S, Pati AK. Evolution of coherence and non-classicality under global environmental interaction. Quantum Inf. Process. 2018;17(9):1-30.

56. Liu Y, Zou H-M, Fang M-F. Quantum coherence and non-Markovianity of an atom in a dissipative cavity under weak measurement. Chin. Phys. B. 2018;27(1):010304.

57. Kurt A, Eryigit R. Noise-induced non-Markovianity. Phys. Rev. A. 2018;98(4):042125.

58. Voss HU. Anticipating chaotic synchronization. Phys. Rev. E. 2000;61(5):5115.

59. Haken H, Strobl G. An exactly solvable model for coherent and incoherent exciton motion. Z. Phys. A. 1973;262(2):135-48.

60. Reineker P. Exciton dynamics in molecular crystals and aggregates: Springer; 1982.

61. Kiely A. Exact classical noise master equations: Applications and connections. EPL. 2021;134(1):10001.

62. Shapiro V, Loginov V. "Formulae of differentiation" and their use for solving stochastic equations. Phys. A: Stat. Mech. Appl. 1978;91(3-4):563-74.

63. Bourret R, Frisch U, Pouquet A. Brownian motion of harmonic oscillator with stochastic frequency. Physica. 1973;65(2):303-20.

64. de Oliveira MM, Alves SG, Ferreira SC. Continuous and discontinuous absorbing-state phase transitions on Voronoi-Delaunay random lattices. Phys. Rev. E. 2016;93(1):012110.

65. Zhang P. Nonbacktracking operator for the Ising model and its applications in systems with multiple states. Phys. Rev. E. 2015;91(4):042120.

66. Chen B, Fei S-M. Notes on modified trace distance measure of coherence. Quantum Inf. Process. 2018;17(5):1-9.

67. Yang L-M, Chen B, Fei S-M, Wang Z-X. Ordering states with various coherence measures. Quantum Inf. Process. 2018;17(4):1-10.

68. Cai X, Zheng Y. Non-Markovian decoherence dynamics in nonequilibrium environments. J. Chem. Phys. 2018;149(9):094107.

69. Levi F, Mostarda S, Rao F, and Mintert F. Quantum mechanics of excitation transport in photosynthetic complexes: a key issues review. Rep. Prog. Phys. 2015;78:082001.

70. Mahdi M N, Kurt A, Altintas, F. Quantum Coherence and non-Markovianity in a Noisy Quantum Tunneling Problem. quant-ph. arXiv:2208.07947.

71. Cai X, Zheng Y. Decoherence induced by non-Markovian noise in a nonequilibrium environment. Phys. Rev. A. 2016;94(4):042110.

72. Jang S, Menucci B. Delocalized excitons in natural light-harvesting complexes. Rev. Mod. Phys. 2018;90:035003.

73. Goychuk I, Hänggi. Quantum dynamics in strong fluctuating fields. Adv. Phys. 2005;54:525.